Mn-doped silicon nanowires: First-principles calculations

G. Giorgi,[1] X. Cartoixà,[2] A. Sgamellotti,[1] and R. Rurali[2]
[1]*Dipartimento di Chimica, Università di Perugia, 06213 Perugia, Italy*
[2]*Departament d'Enginyeria Electrònica, Universitat Autònoma de Barcelona, 08193 Bellaterra, Spain*
(Received 11 April 2008; revised manuscript received 3 September 2008; published 30 September 2008)

We present first-principles calculation of Mn-doped silicon nanowires. We discuss the energetics of both isolated point defects and Mn dimers, where a different behavior of the magnetization vs doping curve is predicted depending on the type of impurity. As a result of the broadening of the band gap, the range of doping condition that favors the stability of the substitutional Mn defect increases with respect to bulk. We also show that Mn dimers favor ferromagnetic alignment, discussing how the driving force to form aggregates has an essential role to stabilize ferromagnetism in the nanowires.

DOI: 10.1103/PhysRevB.78.115327 PACS number(s): 75.75.+a, 73.22.−f, 75.50.Pp

Recently, dilute magnetic semiconductors (DMSs) have attracted much attention for the wide applicability of their chemical and physical properties in spintronics.[1,2] The reported ferromagnetism (FM) of this class of compounds[3] due to the presence of transition metal impurities couples well with the properties of electronic transport of traditional semiconductors, thus leading to the development of spin-controlled electronic and integrated magnetic devices, i.e., a high-speed device structure.[1] After the success gained with the II-VI (Ref. 4) and III-V (Ref. 5) compounds, the focus has been extended to the analysis of group-IV-based DMSs.[6,7] In particular, moving from the encouraging results about ferromagnetic Mn_xGe_{1-x},[8] the properties of similar compounds such as Mn_xSi_{1-x} have been investigated, although nowadays they still remain a matter of theoretical and experimental debate. Techniques based on molecular beam epitaxy have been employed in order to highly dope Si with Mn (about 5%).[9,10] Magnetron cosputtering has been used as well for the deposition of Mn-doped Si thin films[11] on Si substrates. The initial film is amorphous, whereas once annealed at 800 °C it is single-phase polycrystalline with a room-temperature FM behavior.

A further challenge is the achievement of DMSs at the nanoscale.[12–14] Besides the intrinsic interest for future nanoelectronic applications, nanostructures can behave much differently from their bulk counterparts. Wang *et al.*,[15] for instance, have shown that the magnetic coupling in Mn-doped GaN nanowires is ferromagnetic unlike that in the thin film. Very recently, Wu *et al.*[16] have reported the room-temperature FM of Mn-implanted Si nanowires (SiNWs) grown through chemical vapor deposition. In particular, they observe a linear dependence of the saturation magnetization on the Mn concentration after annealing at 600 °C; at 800 °C annealing FM disappears and Mn atoms segregate to the surface of the nanowires. Aiming at combining both analysis on one-dimensional systems with that of magnetism in DMSs, we performed *ab initio* calculations in order to find out the preferential site of implantation of a Mn impurity in a SiNW with a diameter of approximately 1.5 nm oriented along the ⟨111⟩ axis, which is a very common growth orientation. The analysis has been extended to the magnetism of Mn dimers. We compare our results with the first-principles calculations of energetics of Mn in bulk obtained by Bernardini *et al.*[6] where, in agreement with experimental results, the existence of an energy-driven force for Mn to aggregate and form dimers was demonstrated. The obtained results reveal that aggregation is still favored in SiNWs and plays a significant role in stabilizing the system ferromagnetism.

We have performed spin-polarized first-principles calculations in the framework of density-functional theory as implemented in the SIESTA package.[17] We have used norm-conserving pseudopotentials of the Troullier-Martins type[18] for the core electrons, an optimized double-ζ polarized basis set,[19,20] and the generalized gradient approximation (GGA) (Ref. 21) for the exchange and correlation energy. We have used a large ⟨111⟩ SiNW supercell (c-axis lattice parameter 18.81 Å) to guarantee that there is enough separation between the impurity and its periodic images (16.5 Å has proven to be sufficient for bulk Si)[6] and a k-point sampling of $(1\times1\times4)$ according to the Monkhorst-Pack algorithm.[22] We have relaxed the positions of all the atoms until the maximum force was lower than 0.04 eV/Å, with no constraint either on the atomic coordinates or on the overall symmetry of the wire. The equilibrium lattice parameter in thin SiNWs is known to exhibit some deviations from the one of the bulk;[23] thus, the ⟨111⟩ axial lattice parameter has been obtained from a separate calculation of the pristine wire where the cell vectors have been optimized together with the atomic coordinates. For consistency with Bernardini *et al.*[6] the reference phase of Mn used to define its chemical potential was the antiferromagnetic (AFM) fcc metallic structure. We have considered the ±2, ±1, and 0 charge states for all defects. Introducing a point charge within a periodic boundary-condition scheme would result in a divergent electrostatic energy. A common way to avoid this problem is using a uniform neutralizing background and applying *a posteriori* the Madelung correction to the total energy of the charged systems.[24] This formalism, originally proposed for molecules and bulk systems, has to be properly generalized for one-dimensional systems,[25] where one must take into account the difference between the axial and transverse dielectric constants and generic cells shapes (the transverse dimensions of the supercell being normally much larger than the axial length).

At first, we have studied isolated Mn impurities with the purpose of elucidating which configurations are most stable. We have considered: (i) substitutional manganese Mn_{Si}; (ii) tetragonal interstitial manganese Mn_i^T, where the Mn atom

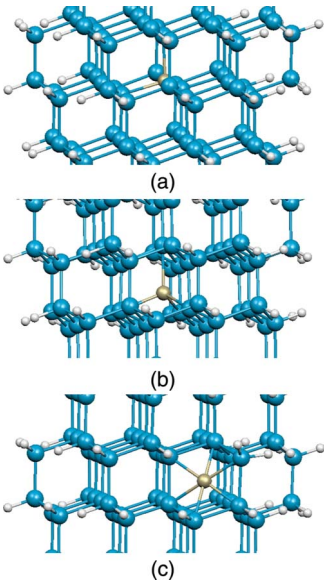

FIG. 1. (Color online) Point defects studied. (a) Substitutional manganese Mn_{Si}, (b) tetragonal interstitial manganese Mn_i^T, and (c) hexagonal interstitial manganese Mn_i^H. Mn atoms are represented by a light golden sphere, whereas for Si and H we use dark blue and white spheres, respectively.

occupies an interstitial position with four Si first neighbors; and (iii) hexagonal interstitial manganese Mn_i^H, where the Mn atom occupies an interstitial position with six Si first neighbors. The structures are shown in Fig. 1. For each one of these configurations we have calculated the formation energy as a function of the Fermi energy,[25,26] taking into account the proper potential lineup,[27] although it results in a marginal correction. The results are shown in Fig. 2. We have found a general agreement with the results obtained by Bernardini *et al.*[6] for *n*-doped bulk Si although some important differences arise for *p*-type doping. As in bulk, in the ⟨111⟩ SiNW the most stable defect for low values of the electron chemical potential is the Mn_i^T. For *n*-type doping (i.e., high values of the electron chemical potential) Mn_{Si} prevails. A similar situation was observed for bulk Si.[6] However, an important difference is that Mn_{Si} already becomes the most stable point defect for values of the electron chemical potential around midgap, while for bulk Si the inversion of stability occurred only in the very end of the spanned range of Fermi energies. Also, the substitutional is ~0.7 eV more stable than Mn_i^T for values of the electron chemical potential close to its upper limit; while in bulk the difference was much lower, leading Bernardini *et al.*[6] to suggest a possible coexistence of the two defects. For *p*-doping conditions the difference in formation energies is about 1 eV. However, when E_F is close to the top of the valence band (E^{TVB}) the Mn_i^H, not considered in the analysis of Ref. 6, is favored over the Mn_{Si}, thus lowering the difference of formation energy between the most stable and the next most stable defects. For both Mn_{Si} and Mn_i^T the T_d symmetry is maintained with first neighbors at 2.35–2.37 and 2.41–2.47 Å, respectively. The relaxation of Mn_i^H is more complicated and the six atoms that should ideally be first neighbors are at slightly different distances from the Mn impurity; this is an effect of the proximity of the *H* interstitial position (the only one available) to the surface which makes the six first neighbors highly nonequivalent. Also, we should note that in some cases Mn_i^H relaxes in the course of the conjugate gradient (CG) optimization to a Mn_i^T position, indicating that the migration barrier is very low.

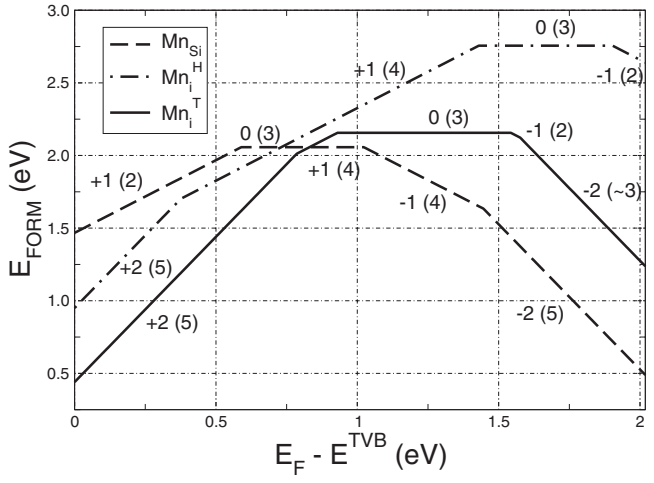

FIG. 2. Formation energies of Mn point defects in 1.5 nm ⟨111⟩ SiNW. The electron chemical potential is referred to the top of the valence band and varies throughout the GGA band gap, which is known to be an underestimation. Hybrid-functional calculation estimates a band gap of 2.35 eV for this wire (Ref. 28). The charge state and the total magnetization in units of the Bohr magneton μ_B (in parentheses) are indicated in the figure.

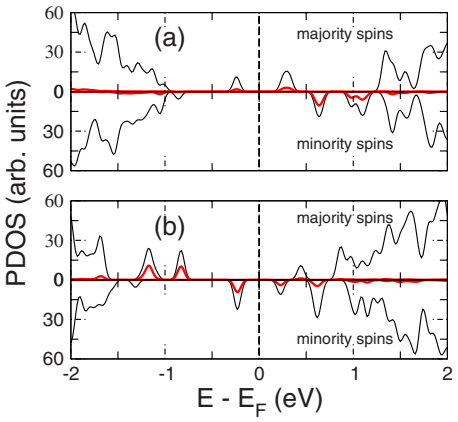

FIG. 3. (Color online) Density of states projected over Mn impurities (thin red line) for majority and minority spins for charge neutral (a) substitutional impurity and (b) tetragonal interstitial. The total DOS is also shown for reference (thick black line).

It is interesting to observe that the defects considered have a rather different population distribution between majority and minority spins (see Fig. 3). Neutral Mn_{Si} has a total magnetization of $3\mu_B$, where μ_B is the Bohr magneton, and both the highest occupied and lowest unoccupied Mn levels have majority spins [Fig. 3(a)]. Therefore, a negative charging of the defects, i.e., Mn_{Si}^-, results in an increase in the magnetization to 4, while Mn_{Si}^+ will have a magnetization of 2. On the other hand, in the case of the tetragonal interstitial [Fig. 3(b)] both the last occupied and first empty elec-

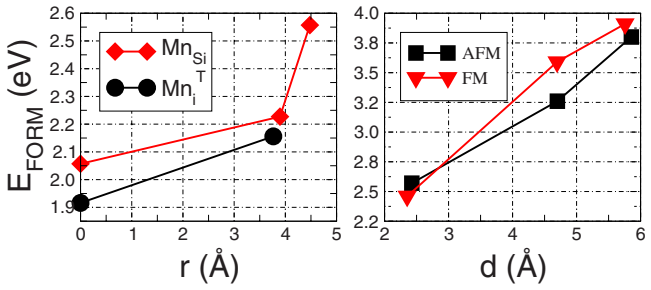

FIG. 4. (Color online) Left panel: Formation energy of neutral Mn_{Si} and neutral Mn_i^T as a function of their radial coordinate (r=0 meaning at the center of the wire). Right panel: Formation energy of the Mn_{Si}-Mn_i^T as a function of their separation d. Mn atoms favor FM alignment only when they are first neighbors.

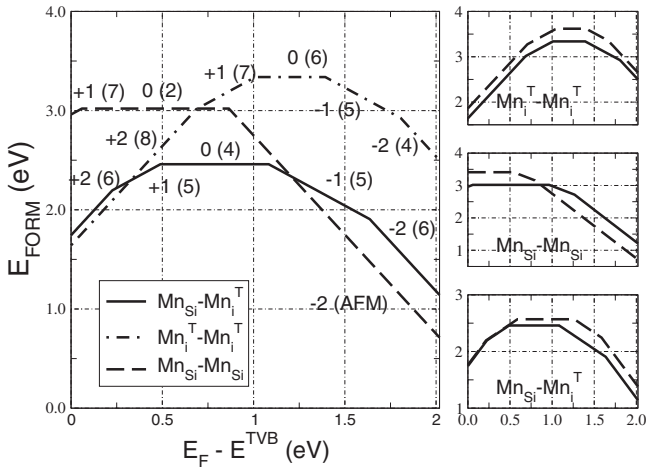

FIG. 5. Pair formation energies of Mn complexes. In the side panel the formation energy of the FM (continuous line) and the AFM case (dashed line) is shown for each Mn-complex.

tronic states are minority Mn states. This results in a different response of the magnetization as a function of the Fermi-level position. Here Mn_i^{T-} has a lower magnetization because an extra minority-spin state is populated, whereas Mn_i^{T+} has a higher magnetization as a minority-spin state is depleted. As discussed above (Fig. 2), the overall doping condition of the wire determines the charge state of each defect and, consequently, its magnetization. From the combined observations of Fig. 2 and Fig. 3 we predict that an increase in the magnetization as the Fermi level moves toward the conduction band is a clear signature of substitutional defects. On the other hand, if the magnetization decreases as the wire turns more and more n type, the defect most abundantly present is an interstitial. In the hexagonal interstitial Mn_i^H (not shown) the dependence of the magnetization on the charge state follows the same pattern than with Mn_i^T; but now, the localized Mn peaks are broadened by the larger interaction with Si first neighbors.

At variance with bulk, SiNWs have translational symmetry only along the wire axis and the lattice sites are not radially equivalent. Common doping impurities, such as B and P, have proven to favor surface segregation in SiNWs,[29,30] which has potential negative implications concerning the doping efficiency (dopants can then get easily passivated at the surface). We have, therefore, checked the dependence of the formation energy of Mn_{Si} and Mn_i^T with the impurity radial coordinate.[31] We have found (see Fig. 4) a slight tendency for both Mn defects to stay at the center of the wires. This finding is apparently at odds with the experimental results of Wu *et al.*[16] (see the discussion below), where out diffusion is believed to take place after high-temperature annealing.

We now turn our attention to Mn complexes and to their preferential magnetic ordering. We have studied substitutional pairs Mn_{Si}-Mn_{Si}, tetragonal interstitial pairs Mn_i^T-Mn_i^T, and substitutional-interstitial pairs Mn_{Si}-Mn_i^T. These pairs are constituted by first-neighboring impurities. All these complexes are stable and FM ordering is largely dominant (Fig. 5). The noticeable exception is represented by the double substitutional Mn_{Si}-Mn_{Si} where AFM ordering is favored for n-doping conditions. For p-type and neutral dopings the dimers align their magnetic momenta ferromagnetically, with the Mn_{Si}-Mn_i^T prevailing over other complexes, except for Fermi energies very close to the valence-band edge where a coexistence with Mn_i^T-Mn_i^T, although still FM, is expected.

All these pairs—both in the FM and AFM alignments—exhibit a tendency to favor aggregation, in agreement with the results reported for bulk Si.[6] The aggregation tendency might seem an unfortunate occurrence as in principle it is not compatible with the design of doping profiles and uniform impurity distribution. An uncontrolled aggregation would create Mn islands, making the use of the host semiconductor for spintronic applications troublesome. In this case, however, aggregation acts as a stabilizer of the FM ordering. For the dominant aggregate among those considered, Mn_{Si}-Mn_i^T, we have studied the dependence of the FM/AFM energy on the Mn-Mn separation. Figure 4 shows that only when the impurities are first neighbors they align their magnetic moment ferromagnetically, favoring AFM ordering otherwise. Therefore, although clustering is in principle an undesired event, in the case of Mn in SiNWs, it appears to be necessary to have FM-ordered dimers. Of course it is still possible that, although the Mn atoms of one dimer align ferromagnetically, the dimer-to-dimer coupling is absent or AFM. To rule out this possibility we have studied *two* different Mn_{Si}-Mn_i^T complexes in the same wire. We know that each dimer favors FM order, i.e., $\uparrow\uparrow$, but this setup allowed us to consider explicitly the $\uparrow\uparrow\uparrow\uparrow$ and the $\uparrow\uparrow\downarrow\downarrow$ ordering. The $\uparrow\uparrow\uparrow\uparrow$ FM phase turned out to 0.14 eV more stable than the $\uparrow\uparrow\downarrow\downarrow$ paramagnetic phase, indicating that once the short-range alignment is established, $\uparrow\uparrow$ dimers favor an alignment of their magnetic momenta, too.

Room-temperature magnetism in Mn-doped SiNWs was reported in the work of Wu *et al.*[16] after annealing their ion-implanted SiNWs:Mn at 600 °C. On the other hand, annealing at 800 °C was observed to destroy the FM character. We propose the following explanation for these observations. Interstitial impurities are more mobile defects than substitutionals. (Gilles *et al.*[32] showed that Mn diffusivity is strongly reduced for n-doped samples as Mn substitutionals become more abundant than interstitials.[6]) Then, noting that the complexes that promote FM always include at least one intersti-

tial Mn, the 600 °C temperature might be high enough to allow the formation of FM-coupled pairs but low enough to prevent the onset of other processes. The reason for the loss of the magnetism in the SiNWs when the annealing temperature is set to 800 °C is less clear, and more experiments are needed to clarify that process. Our calculations suggest two possible mechanisms: (a) Double substitutionals can now form and, for certain doping conditions, they favor AFM coupling. (b) Uncontrolled aggregation occurs and large single domain uncorrelated Mn clusters form. The formation of large Mn clusters is compatible with the observations in Ref. 16, although further experimental work is needed to fully clarify this point. According to this scenario, the aggregates observed on the surface of the wires[16] are not precipitates resulting from Mn segregation but rather Mn clusters that form throughout the wire section which are only visible on the surface.

Incidentally, we note that surface segregation would not be consistent with our calculations that indicate a moderate tendency for Mn impurities to remain in the core of the wires. If surface segregation were indeed experimentally observed, this discrepancy might be due to a variety of effects not taken into account here, such as transient enhanced diffusion[33] or cluster diffusion.[34]

In summary, we have studied Mn impurities in ⟨111⟩ SiNWs. The most stable Mn point defect turns out to be the tetragonal interstitial for most of the doping conditions, while substitutional Mn is favored for *n* doping similarly to bulk silicon. Mn dimers are stable and their formation is energetically favored. Such spontaneous aggregation turns out to play a central role in the stabilization of FM ordering, because as the separation between two Mn impurities grows the AFM phase becomes more stable. Comparison with experimental results suggests that at too high annealing temperatures uncontrolled clustering—or other enhanced diffusion mechanism yet to be elucidated—takes place, destroying the magnetism

X.C. and R.R. acknowledge financial support from Spain's Ministry of Education and Science Ramón y Cajal program under Contract No. TEC2006-13731-C02-01. G.G. and A.S. acknowledge support from MIUR (FIRB 2003: Molecular compounds and hybrid nanostructured materials with resonant and nonresonant optical properties for photonic devices).

[1] S. A. Wolf, D. D. Awschalom, R. A. Buhrman, J. M. Daughton, S. von Molnar, M. L. Roukes, A. Y. Chtchelkanova, and D. M. Treger, Science **294**, 1488 (2001).
[2] I. Zutic, J. Fabian, and S. D. Sarma, Rev. Mod. Phys. **76**, 323 (2004).
[3] H. Ohno, Science **281**, 951 (1998).
[4] J. K. Furdyna and J. Kossut, in *Diluted Magnetic Semiconductors*, Semiconductors and Semimetals, edited by R. K. Willardson and A. C. Beer (Academic, New York, 1988), Vol. 25.
[5] H. Ohno, A. Shen, F. Matsukura, A. Oiwa, A. Endo, S. Katsumoto, and Y. Iye, Appl. Phys. Lett. **69**, 363 (1996).
[6] F. Bernardini, S. Picozzi, and A. Continenza, Appl. Phys. Lett. **84**, 2289 (2004).
[7] J. T. Arantes, A. J. R. da Silva, A. Fazzio, and A. Antonelli, Phys. Rev. B **75**, 075316 (2007).
[8] Y. D. Park, A. T. Hanbicki, S. C. Erwin, C. S. Hellberg, J. M. Sullivan, J. E. Mattson, T. F. Ambrose, A. Wilson, G. Spanos, and B. T. Jonker, Science **295**, 651 (2002).
[9] H. Nakayama, M. Ohta, and E. Kulatov, Physica B **302-303**, 419 (2001).
[10] S. Abe, Y. Nakasima, S. Okubo, H. Nakayama, T. Nishino, H. Yanagi, and H. Ohta, Appl. Surf. Sci. **142**, 537 (1999).
[11] L. Liu, N. Chen, Y. Wang, Z. Yin, F. Yang, C. Chai, and X. Zhang, J. Cryst. Growth **291**, 239 (2006).
[12] D. Neumaier, K. Wagner, S. Geißler, U. Wurstbauer, J. Sadowski, W. Wegscheider, and D. Weiss, Phys. Rev. Lett. **99**, 116803 (2007).
[13] T. M. Schmidt, P. Venezuela, J. T. Arantes, and A. Fazzio, Phys. Rev. B **73**, 235330 (2006).
[14] J. T. Arantes, A. J. R. da Silva, and A. Fazzio, Phys. Rev. B **75**, 115113 (2007).
[15] Q. Wang, Q. Sun, and P. Jena, Phys. Rev. Lett. **95**, 167202 (2005).
[16] H. W. Wu, C. J. Tsai, and L. J. Chen, Appl. Phys. Lett. **90**, 043121 (2007).
[17] J. M. Soler, E. Artacho, J. D. Gale, A. García, J. Junquera, P. Ordejón, and D. Sánchez-Portal, J. Phys.: Condens. Matter **14**, 2745 (2002).
[18] N. Troullier and J. L. Martins, Phys. Rev. B **43**, 1993 (1991).
[19] E. Anglada, J. M. Soler, J. Junquera, and E. Artacho, Phys. Rev. B **66**, 205101 (2002).
[20] V. Ferrari, J. M. Pruneda, and E. Artacho, Phys. Status Solidi A **203**, 1437 (2006).
[21] J. P. Perdew, K. Burke, and M. Ernzerhof, Phys. Rev. Lett. **77**, 3865 (1996).
[22] H. J. Monkhorst and J. D. Pack, Phys. Rev. B **13**, 5188 (1976).
[23] T. Vo, A. J. Williamson, and G. Galli, Phys. Rev. B **74**, 045116 (2006).
[24] G. Makov and M. C. Payne, Phys. Rev. B **51**, 4014 (1995).
[25] R. Rurali and X. Cartoixà, arXiv:0806.1847 (unpublished).
[26] S. B. Zhang and J. E. Northrup, Phys. Rev. Lett. **67**, 2339 (1991).
[27] S. Pöykkö, M. J. Puska, and R. M. Nieminen, Phys. Rev. B **53**, 3813 (1996).
[28] R. Rurali, B. Aradi, T. Frauenheim, and A. Gali, Phys. Rev. B **76**, 113303 (2007).
[29] M. V. Fernández-Serra, C. Adessi, and X. Blase, Phys. Rev. Lett. **96**, 166805 (2006).
[30] T. Markussen, R. Rurali, A.-P. Jauho, and M. Brandbyge, Phys. Rev. Lett. **99**, 076803 (2007).
[31] SiNWs grown along the ⟨111⟩ crystallographic axis have no radial symmetry. When we define a defect by its radial coordinate we just want to give a rough measure of how far from the surface it is, whereas we do not imply that defects with the same radial coordinate are symmetrically equivalent.

[32] D. Gilles, W. Schröter, and W. Bergholz, Phys. Rev. B **41**, 5770 (1990).
[33] P. A. Stolk, H.-J. Gossmann, D. J. Eaglesham, D. C. Jacobson, C. S. Rafferty, G. H. Gilmer, M. Jaraíz, J. M. Poate, H. S. Luftman, and T. E. Haynes, J. Appl. Phys. **81**, 6031 (1997).
[34] S. K. Estreicher, M. Gharaibeh, P. A. Fedders, and P. Ordejón, Phys. Rev. Lett. **86**, 1247 (2001).